Molecular Neurobiology
https://doi.org/10.1007/s12035-020-02008-y

Differential Effect of Repeated Lipopolysaccharide Treatment and Aging on Hippocampal Function and Biomarkers of Hippocampal Senescence

Jolie Barter[1] · Ashok Kumar[2] · Asha Rani[2] · Luis M Colon-Perez[3] · Marcelo Febo[2,4,5] · Thomas C. Foster[2,6]

Received: 13 February 2020 / Accepted: 1 July 2020

Abstract

Markers of brain aging and cognitive decline are thought to be influenced by peripheral inflammation. This study compared the effects of repeated lipopolysaccharide (LPS) treatment in young rats to age-related changes in hippocampal-dependent cognition and transcription. Young Fischer 344 X Brown Norway hybrid rats were given intraperitoneal injections once a week for 7 weeks with either LPS or vehicle. Older rats received a similar injection schedule of vehicle. Old vehicle and young LPS rats exhibited a delay-dependent impairment in spatial memory. Further, LPS treatment reduced the hippocampal CA3–CA1 synaptic response. RNA sequencing, performed on CA1, indicated an increase in genes linked to neuroinflammation in old vehicle and young LPS animals. In contrast to an age-related decrease in transcription of synaptic genes, young LPS animals exhibited increased expression of genes that support the growth and maintenance of synapses. We suggest that the increased expression of genes for growth and maintenance of synapses in young animals represents neuronal resilience/recovery in response to acute systemic inflammation. Thus, the results indicate that repeated LPS treatment does not completely recapitulate the aging phenotype for synaptic function, possibly due to the chronic nature of systemic inflammation in aging and resilience of young animals to acute treatments.

Keywords Inflammation · LPS · Hippocampus · Synaptic function · Cognition · NMDA receptor

Introduction

It is well established that the immune system can modulate brain function. Understanding how inflammation alters neural function is important for aging research, since aging is associated with reduced functional ability of the immune system [1] and elevated systemic markers of inflammation [2, 3]. In turn, elevated systemic inflammation in adults is associated with greater cognitive decline examined years later [4, 5]. Potential mechanisms for systemic inflammation influences on the brain include direct effects of cytokines, increased oxidative stress, activation of glial cells, and impaired synaptic function. Similarly, the aged brain is characterized by increased markers of neuroinflammation [6, 7], altered redox state [8, 9], and a decrease in the N-methyl-D-aspartate receptor (NMDAR)-mediated component of synaptic transmission [10, 11].

The goal of the current study was to determine if repeated injections of lipopolysaccharide (LPS) result in cognitive impairments and hippocampal changes that mimic an aged brain. LPS increases markers of systemic inflammation and does not cross the blood brain barrier [12]; therefore, LPS has often been employed to study the relationship between peripheral inflammation and cognition [13]. In the current study, LPS was injected once a week, for 7 weeks. Similar to aging, LPS injections resulted in a decline in hippocampal-dependent spatial episodic memory. Memory impairment was evident several days following the last treatment,

Electronic supplementary material The online version of this article (https://doi.org/10.1007/s12035-020-02008-y) contains supplementary material, which is available to authorized users.

✉ Thomas C. Foster
foster1@ufl.edu; Kash@ufl.edu

[1] Department of Medicine, Division of General Medicine and Geriatrics, Emory University School of Medicine, Atlanta, GA, USA

[2] Department of Neuroscience, McKnight Brain Institute, University of Florida, Gainesville, FL 32610-0244, USA

[3] Department of Neurobiology and Behavior, Center for Learning and Memory, University of California, Irvine, CA 92697, USA

[4] Department of Psychiatry, McKnight Brain Institute, University of Florida, Gainesville, FL, USA

[5] Center for Addiction Research and Education, University of Florida, Gainesville, FL 32611, USA

[6] Genetics and Genomics Program, University of Florida, Gainesville 32611, FL, USA

Published online: 10 July 2020

suggesting long-term effects. LPS injections were associated with an increase in expression of inflammation-related genes in the hippocampus and a decrease in hippocampal synaptic transmission, including a decline in the NMDAR-mediated component of synaptic transmission. In contrast to aging, young LPS-treated animals exhibited increased transcription of synaptic component genes several days following the last injection. The results indicate that peripheral inflammation can drive impaired memory and some markers of brain aging. However, young animals may exhibit compensatory transcriptional mechanisms, which may permit recovery of hippocampal function.

Methods

Animals

Young ($n = 54$, 5–7 months) and older, approximately middle-age ($n = 9$, 14–16 months) male Fischer 344 X Brown Norway hybrid rats were obtained from the National Institute on Aging colony through the University of Florida Animal Care and Service facility. Animals were housed in pairs on a 12:12 light/dark cycle (lights on at 6 PM). All procedures involving animals were approved by the Institutional Animal Care and Use Committee at the University of Florida and were in agreement with guidelines recognized by the U.S. Public Health Service Policy on Humane Care and Use of Laboratory Animals. Animals were handled for 1 week before any testing occurred to allow for acclimation to the new environment. Animals were weighed once per week before receiving intraperitoneal injection of vehicle or LPS (1 mg/kg; Sigma catalog number L4524 isolated from *Escherichia coli* serotype O55:B5 and purified form ion exchange). For behaviorally characterized animals, the weight prior to the first injection was used as a baseline for calculating the percent change in weight over the course of the experiment. In a separate subset of animals (young vehicle $n = 4$; young LPS $n = 6$), changes in weight were recorded across the 6 weeks of treatment and temperature was assessed by rectal probe at time points 0, 4, 24, 48, and 72 h after the first and sixth injections.

Electrophysiology

Figure 1a illustrates the experimental timeline to assess if repeated LPS injections changed hippocampal synaptic function. These animals were not behaviorally characterized; rather, young animals were injected with LPS ($n = 8$) or vehicle ($n = 8$) once a week for 6 weeks. Hippocampal slices were prepared 24 ($n = 4$ per group) or 72 ($n = 4$ per group) hours following the last LPS or vehicle injection. Methods for collection of hippocampal slices and recordings have been published previously [10, 14–16]. Briefly, rats were anesthetized with isoflurane (Halocarbon Laboratories, River Edge, NJ) and decapitated. Brains were rapidly removed and hippocampi were dissected. Hippocampal slices (~400 μm) were cut parallel to the Alvear fibers using a tissue chopper. Slices were incubated in a holding chamber (room temperature) containing standard artificial cerebrospinal fluid (aCSF) (in mM): NaCl 124, KCl 2, KH_2PO_4 1.25, $MgSO_4$ 2, $CaCl_2$ 2, $NaHCO_3$ 26, and glucose 10. Thirty to sixty minutes before recording, 2–3 slices were transferred to a standard interface recording chamber (Harvard Apparatus, Boston, MA). The chamber was continuously perfused with standard oxygenated (95% O_2, 5% CO_2) aCSF at a flow rate of 2 ml/min. The pH and temperature were maintained at 7.4 and 30 ± 0.5 °C, respectively. Humidified air (95% O_2, 5% CO_2) was continuously blown over the slices.

The total extracellular synaptic field potential (total fEPSP) from CA3–CA1 hippocampal synaptic contacts were recorded with a glass micropipette (4–6 MΩ) filled with aCSF. Concentric bipolar stimulating electrodes (outer pole: stainless steel, 200-μm diameter; inner pole: platinum/iridium, 25-μm diameter, Fredrick Haer & Co, Bowdoinham, ME) were positioned approximately 1 mm from the recording electrode localized to the middle of stratum radiatum to stimulate CA3 inputs onto CA1. Using an SD9 stimulator (Grass Instruments), field potentials were induced by single diphasic stimulus pulses (100 μs). Signals were amplified, filtered between 1 and 1 kHz, and stored on computer disk for off-line analysis (Data Wave Technologies, Longmont, CO). The NMDAR-mediated component of synaptic transmission (NMDAR fEPSP) was obtained by incubating the slices in aCSF that contained low magnesium (Mg^{2+}) (0.5 mM), 6,7-dinitroquinoxaline-2,3-dione (DNQX, 30 μM), and picrotoxin (PTX, 10 μM) [10]. Input-output curves for the total and NMDAR fEPSP (mV/ms) were constructed for increasing stimulation intensities.

The effect of the reducing agent, dithiothreitol (DTT, 0.5 mM), on the NMDAR fEPSP was examined by setting a baseline response at 50% of the maximum and responses were collected for at least 10 min before (i.e., baseline) and 60 min after DTT application.

Spatial Water Maze

Figure 1b illustrates the experimental timeline used to assess the effect of LPS on spatial learning and memory. One week following arrival, young ($n = 28$) and older ($n = 9$) animals were behaviorally pre-tested on the cue and spatial versions of the water maze task. Pre-testing was performed to familiarize the animals with the procedural aspects of the task and ensure that older animals were not impaired in their ability to acquire a spatial search strategy. The water was dyed white (Rich Art-Tempera Paint) and animals were tracked on Noldus Ethovision computer software (Noldus Information

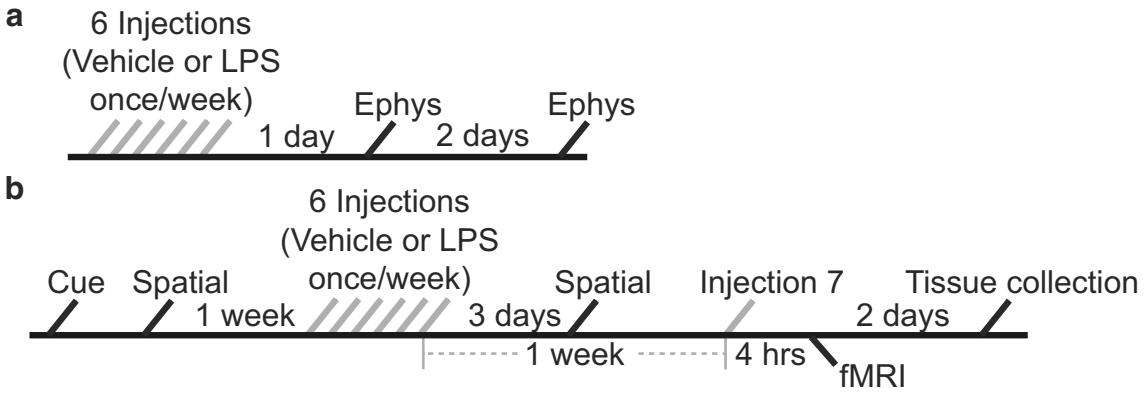

Fig. 1 Schematic representing the experimental paradigms. **a** Young rats were either injected with vehicle ($n = 8$) or LPS ($n = 8$) once a week for 6 weeks. Total and NMDA receptor–mediated synaptic transmission were examined 24 ($n = 4$ per treatment group) or 72 h after the final injection ($n = 4$ per treatment group). **b** Young ($n = 28$, 5–7 months) and older ($n = 9$, 14–16 months) rats were first prescreened on the cue and spatial discrimination water maze task. Young rats were divided to receive either 6 injections once a week with vehicle ($n = 13$) or LPS ($n = 15$). Older rats received 6 weeks of vehicle injections. Three days after the 6th injection, animals were cognitively assessed on the spatial discrimination water maze task. A final (7th) injection of vehicle or LPS was given 1 week after the 6th injection. fMRIs were performed 4 h after the final injection in a subset of young vehicle ($n = 8$) and young LPS ($n = 8$) rats. Tissue was collected 2 days after the final injection

Technology, Leesburg, VA, USA). The pool was surrounded by a black curtain in order to control spatial cues. First, animals were habituated to the pool by freely swimming for 30 s with gentle guidance to the platform. Following habituation, the cue version of the water maze was performed to assess sensory-motor performance. The platform was set at 1 cm above the water level and topped with a white flag. Cue training consisted of five blocks of three trials (15 total trials) massed into a single day. Each trial consisted of a randomly assigned platform position and release point. For each trial, the animal was placed into the water and given 60 s to find the platform. If unsuccessful, the animal was gently guided to the platform.

Three days after cue training, the animals were tested on the 1-day version of the spatial water maze, according to previously described methods [17, 18]. Briefly, the flag was removed and the platform was submerged 1.5 cm under the water level and remained in the same location throughout all trials. Large objects were attached to the black curtain to act as extra-maze cues. Each trial consisted of a randomly assigned release point. If the animal did not find the platform within 60 s, it was gently guided to the platform. The spatial discrimination training consisted of 5 training blocks of three trials (15 total trials). An acquisition probe trial was inserted between blocks 4 and 5 to assess if animals had acquired a spatial search strategy. During the probe trial, the platform was removed and the animal was released from the quadrant opposite the goal. The animal was allowed to swim for 30 s and the time spent in the goal and opposite quadrants was recorded. Following the acquisition probe trial, a refresher-training block was performed (block 5).

To examine the effects of LPS on memory, young animals were injected with vehicle ($n = 13$) or LPS ($n = 15$) once a week for 6 weeks. All older animals ($n = 9$) received vehicle injections. Starting 72 h after the sixth injection, the spatial version of the task was repeated, with the escape platform located to a new quadrant. In addition, a memory retention probe trial was delivered 2 h after the acquisition probe trial. Performance on the probe trials was analyzed using a discrimination index (DI) score, which measures time spent in the goal quadrant compared with the time in the opposite quadrant [(Goal Quadrant − Opposite Quadrant)/(Goal Quadrant + Opposite Quadrant)].

Functional Magnetic Resonance Imaging

A subset of behaviorally characterized young animals (vehicle $n = 8$; LPS $n = 8$) were imaged 4 h after the final injection (injection 7). Similar to previously published methods [19–21], rats were imaged after low doses of dexmedetomidine (0.02 mg/kg) and isoflurane (0.5%) anesthesia. Spontaneous breathing rates and core body temperature were monitored during the MRI scan (SA Instruments, Stony Brook, NY). A water recirculation system was used to maintain a core body temperature at 37–38 °C (Gaymar, Brentwood, MO). Images were collected on a 4.7-T/33-cm horizontal magnet (Magnex Scientific, Yarnton, UK) with an 11.5-cm-diameter gradient insert (670-mT/m maximum gradient strength at 300 Amps and a 120-μs rise time; Resonance Research) and controlled by VnmrJ 3.1 software (Agilent, Santa Clara, CA). For B1 field excitation and radio frequency (RF) signal detection (Air MRI), a quadrature transmit/receive RF coil tuned to 200.6 MHz 1H resonance was used. To collect functional images, a two-shot spin echo-echo planar imaging (EPI) sequence with the following parameters: echo time (TE) = 50 ms; repetition time (TR) = 1 s;

32.5 × 32.5 mm in-plane; 12 slices with 1.5-mm thickness per slice; data matrix = 64 × 64 was used. There were a total of 210 repetitions per EPI scan (7 min), with two scans per rat. There were no stimuli presented during functional scanning. In the same space as the EPI scan, anatomic scans for image overlay and reference-to-atlas registration were collected using a fast spin echo sequence (TE = 45 ms; TR = 2 s; echo train length = 8; number of averages = 10; data matrix = 256 × 256).

Image Processing and Statistical Analysis

Brain masks were manually created using high-resolution anatomical scans to remove non-brain voxels on itkSNAP (www.itksnap.org). The FMRIB Software Library linear registration program *FLIRT* [22] was used to align cropped brain images to a rat brain template. For each subject, registration matrices were saved and used to transform functional datasets into an atlas space for preprocessing and analysis. Over the series of 210 images, slight displacements in individual images and slice timing delays were corrected. In addition, time-series spikes were removed using Analysis of Functional NeuroImages (AFNI; [23]). Linear and quadratic detrendings, spatial blurring (1.1-mm FWHM), and intensity normalization were applied to all images. Based on their location in the segmented atlas, head motion parameters and cerebroventricular and white matter signals were extracted and removed from datasets. Brain signals that contain higher frequency oscillations were removed by a voxelwise temporal bandpass filter (between 0.01 and 0.1 Hz) before time-series correlation analyses were performed.

Based on the atlas-guided seed location, time-series functional magnetic resonance imaging (fMRI) signals were extracted per each region of interest (ROI) and averaged over hemispheres (75 ROI). The first nine images in each functional time series were not used to avoid unstable fMRI signal intensity variations that are typically found in the initial images. A time series was created for each voxel that was averaged per ROI seed. Then, voxelwise cross correlations were conducted to create a correlation coefficient (Pearson r) maps [21] and the Pearson r coefficients were then subjected to a voxelwise z transformation. Pearson r coefficients were exported for seed-based functional connectivity and network analyses in MATLAB (MathWorks). AFNI was used to generate composite functional connectivity maps for cortical and subcortical seed regions.

Next, we calculated basic graph theory metrics to assess the topology of functional connectivity networks. The Brain Connectivity Toolbox for MATLAB was used to analyze resting-state fMRI data [24]. Symmetrical connectivity graphs were first organized in MATLAB [graph size = $n(n-1)/2$, where n is the number of nodes represented in the graph or 150 ROIs]. Matrix z values were normalized to the highest z score, such that all matrices had edge weight values from 0 to 1. All graph theory metrics were calculated for several density thresholds (denoted as k level) that preserved the top strongest functional connectivity z values per graph (e.g., top 5–40%). Node strength (the sum of edge weights), the average shortest path length (the potential for communication between pairs of structures), clustering coefficient (the degree to which nodes cluster together in groups), modularity (the degree to which the network may be subdivided into clearly delineated groups or communities), and small worldness (the degree to which functional brain networks deviate from randomly connected networks) were calculated for both weighted or unweighted graphs [25–29].

The small world (sw) index was calculated by comparing the functional connectivity networks to an average of 10 null hypothesis networks per rat [30]. Thus, we calculated the ratio for clustering coefficients and path lengths of rat brain relative to null networks. The ratio of clustering coefficients is known as γ and the ratio of average path length is referred to as λ. In the sw network, γ is [mt]1 and λ is close to 1 [29]. The sw parameter is the ratio of γ/λ. Therefore, a sw > 1 indicates a small world topology (typical of real-world networks) and a sw ~ 1 indicates a random network [31]. Brain-Net was used to generate brain networks [32]. Brain 3D networks were generated with undirected edges weights (Eundir) ≥ 0.3. In these rat brain connectomes, the node size and color were scaled by the strength of the node, while edges were scaled by z scores.

For statistical analysis, we first compared global measures of network connectivity. Repeated measures analysis of variances (ANOVAs) compared the effect of LPS treatment on small world coefficients, path length, and clustering coefficient over the different density levels (k levels). After this, we performed one-way ANOVAs on the clustering coefficient, node strength, and node degree for each specific ROI analysis to determine those that were affected by LPS treatment. Statistical information for all significant ROIs can be found in Supplementary Table 1.

Tissue Collection

Rats were anesthetized with isoflurane (Halocarbon Laboratories, River Edge, NJ) and decapitated. Brains were rapidly removed and hippocampi were dissected. One hippocampus was kept whole and used for Western blot analysis. The other hippocampus was subdivided into CA1 and dentate gyrus (DG) for RNA sequencing. All samples were flash-frozen in liquid nitrogen.

Western Blot Analysis

For Western blot analyses (young vehicle $n = 6$, young LPS $n = 5$–6), tissue was sonicated in radio-immunoprecipitation assay (RIPA) buffer (Thermo Fisher, Waltham, MA)

supplemented with phosphatase inhibitors, protease inhibitors, and EDTA (Thermo Scientific). The lysed tissue was centrifuged at 20,000 ×*g* for 10 min at 4 °C. A Pierce BCA protein assay was used to measure protein concentration. Lysates were denatured in Laemmli buffer containing 2-mercaptoethanol (BioRad, Hercules, CA) and boiled. For electrophoresis, proteins (30 μg) and kaleidoscope protein standards (Bio-Rad) were separated on 4–15% Tris-HCl gels (Bio-Rad). Protein was transferred to nitrocellulose membrane (Bio-Rad) and blocked with Odyssey blocking buffer (Li-Cor, Lincoln, NE) for 1 h. Membranes were probed overnight at 4 °C with antibodies synaptophysin (Abcam, Cambridge, UK, ab32127, 1:10,000), post-synaptic density protein 95 (PSD-95) (Invitrogen, Carlsbad, CA, MA1-045, 1:400), β-actin (Cell Signaling, Danvers, MA, 3700S, 1:10,000), NMDAR subunit 1 (GluN1) (Millipore, AB9864, 1:1000), and GAPDH (Abcam, ab9485, 1:10,000; ab8245, 1:5000). Membranes were then incubated with secondary antibodies (IRDye 800CW 1:20,000 and 680LT 1:10,000) for 1 h at room temperature. The membrane was washed with TBST 4 times for 10 min each. Membranes were imaged and quantified on the Odyssey infrared scanner (Li-Cor). Protein expression was analyzed using the Li-Cor image studio. Proteins of interest were normalized to the loading control. GAPDH was employed as a loading control for Western blots of PSD-95 and GluN1. Due to the similarity in molecular weight between synaptophysin (38 kDa) and GAPDH (36 kDa), β-actin (42 kDa) was employed as the loading control for synaptophysin.

RNA, Library Preparation, and Sequencing

The transcriptome was analyzed in the hippocampal subregions CA1 and DG from young vehicle ($n = 8$), young LPS ($n = 8$), and old vehicle ($n = 6$) animals. RNA isolation and DNase digestion were performed with RNeasy Lipid Tissue Mini kit (Qiagen, Hilden, Germany, catalog number 74804) and RNase-Free DNase Set (Qiagen, catalog number 79254). RNA concentration was measured using a NanoDrop 2000 spectrophotometer and the RNA integrity number (RIN) was quantified on a high sensitivity (HS) RNA Screen Tape in an Agilent 2200 Tapestation system. The average RIN values (± SEM) for region CA1 in young vehicle, young LPS, and old vehicle animals were 9.0 ± 0.1, 9.2 ± 0.1, and 9.0 ± 0.1. For the DG, the average RIN values for young vehicle, young LPS, and old vehicle animals were 9.0 ± 0.16, 8.9 ± 0.14, and 8.9 ± 0.07. External RNA Controls Consortium (ERCC) spike-in controls (Thermo Fisher, catalog number 4456740) were added to samples as a performance assessment for library preparation. The Dynabead mRNA DIRECT Micro kit (Thermo Fisher, catalog number 61021) was used to select for poly-(A) mRNA and whole transcriptome libraries were prepared with the Ion Total RNA-seq Kit v2 (Thermo Fisher, catalog number 4475936). Ion Xpress barcodes (Thermo Fisher, catalog number 4475485) were added for multiplex sequencing. Qubit double-stranded DNA HS Assay (Thermo Fisher, catalog number 32851) and HS D1000 Screen Tape in a Tapestation system quantified the concentration and size distribution of the whole transcriptome library. Template preparation was performed using an Ion Chef system and sequenced on an ion proton. ERCC analysis was performed in the Torrent Server with the ERCC analysis plugin. ERCC-spiked samples contained at least 40 transcripts with an R^2 of above 0.9. Each sample contained about 30 million reads of 145-base pair length. The RNA-sequencing data from this study has been uploaded to NCBI's Gene Expression Omnibus under the accession number GSE140685.

Bioinformatics and Statistical Analysis of RNA-Sequencing Data

Data analysis was performed in the Partek Flow server. FASTQ files were trimmed based on quality score and aligned to the rat (rn6) genome using STAR. Gene-level counts were generated and annotated in Partek. Genes were normalized using DESeq2 and genes with an average read count less than 5 were removed [33]. Two different comparisons were made: treatment (young LPS v young vehicle) and age (old vehicle v young vehicle). For each of these comparisons, a $p < 0.025$ was used as a statistical filter to select differentially expressed genes for enrichment analysis [34]. Genes that passed our statistical filter were separated based on the direction of change and submitted to the National Institute of Health (NIH) database for annotation, visualization, and integrated discovery (DAVID) for gene enrichment and functional annotation clustering analysis. For this analysis, the first two significant cellular component (CC) gene ontology (GO) terms, biological process (BP) GO terms, and Kyoto Encyclopedia of Genes and Genomes (KEGG) pathways that were found in separate annotation clusters are reported with a limitation of a Benjamini false discovery rate (FDR) $p < 0.05$. In addition, a more directed analysis was performed due to previous research documenting age-related changes in the transcription of specific GO categories: synapse, inflammatory response, and oxidation-reduction process ($p < 0.05$).

Statistical Analysis for Electrophysiology, Behavior, and Western Blots

In most cases, ANOVAs were employed to examine group differences and Fischer's PLSD test was used for post hoc comparisons ($p < 0.05$). Repeated measures ANOVAs were run across stimulation intensities (12–40 V) for electrophysiological studies and across training trial blocks for behavioral experiments involving cue or spatial discrimination on the water maze. In the case of a group and training trial block

interaction, subsequent ANOVAs were performed within each block to localize differences. In addition, two-tailed one-group/one-sample *t*-tests ($p < 0.05$) were performed to determine if the DI scores were different from what was expected by chance (i.e., DI score = 0).

Results

No animals were lost as a result of age or treatment. Behavioral differences after LPS treatment can be associated with sickness. However, with repeated treatment of LPS, animals exhibit an endotoxin tolerance, due to decreased cytokine release, leading to fewer indicators of sickness behavior [35]. In order to examine possible effects of sickness, a group of non-behaviorally characterized young animals (young vehicle $n = 4$; young LPS $n = 6$) were assessed for changes in body temperature after the 1st and 6th injections to determine the longitudinal effects of repeated exposure of LPS on a physiological measure of sickness. LPS-treated animals exhibited an increase in temperature from 4 to 72 h after the first injection (Supplementary Fig. 1A). After the 6th injection, temperature was not increased above baseline for any of the time points examined. In addition, weight was recorded prior to each injection and weight changes due to LPS treatment were examined across the 6 weeks for young animals that were behaviorally characterized and those examined for temperature changes. A repeated measures ANOVA on the percentage of weight change indicated a significant effect of treatment [$F(1,180) = 59.0$, $p < 0.0001$] and of time [$F(5,36) = 36.4$, $p < 0.0001$]. For each week, *t* tests assessing the change in body weight were performed for each group. The results indicated a decrease in weight only for young LPS animals ($n = 21$) after the first and second injections (Supplementary Fig. 1B). Body weight was increased above baseline for week 4–6 in LPS-treated animals and for weeks 1–6 in young vehicle controls ($n = 17$).

Repeated Exposure of LPS Reduced Hippocampal Synaptic Function

The effect of LPS treatment on hippocampal CA1–CA3 synapses was examined by recording total fEPSP from slices obtained 24 or 72 h after the final injection in young animals. Input-output curves were generated by plotting the slope of total synaptic response across different stimulation intensities for vehicle-treated (24-h time point: $n = 8/4$ slices/animals; 72-h time point: $n = 7/4$ slices/animals) and LPS-treated (24-h time point: $n = 8/4$ slices/animals; 72-h time point: $n = 8/4$ slices/animals) animals. Repeated measures ANOVAs across stimulation intensities indicated an interaction of stimulus intensity X treatment for both time points [24-h time point: $F(7,98) = 4.90$, $p < 0.0001$; 72-h time point: $F(7,91) = 4.95$, $p < 0.0001$] due to decreased synaptic responses of LPS-treated animals at the higher stimulation intensities (Fig. 2(A)).

Following the assessment of the total synaptic response, the NMDAR-mediated synaptic component was pharmacologically isolated. Input-output curves were generated for vehicle-treated (24-h time point: $n = 8/4$ slices/animals; 72-h time point: $n = 7/4$ slices/animals) and LPS-treated (24-h time point: $n = 8/4$ slices/animals; 72-h time point: $n = 7/4$ slices/animals) animals. Similar to the total synaptic response, there was an interaction of intensity X treatment [24-h time point: $F(7,98) = 7.40$, $p < 0.0001$; 72-h time point: $F(7,84) = 3.50$, $p < 0.01$] (Fig. 2(B)). Again, this effect was due to decreased NMDAR-mediated synaptic response in LPS-treated animals compared with vehicle.

A decrease in the NMDAR-mediated component of synaptic transmission during aging is due, at least in part, to increased oxidative stress [16, 36]. To determine if the decrease in the NMDAR-mediated response in LPS-treated animals was due to oxidative stress, the reducing agent, DTT, was added to the bath and the response was followed for 1 h. A two-way ANOVA on the increase in the NMDAR synaptic response, 1 h after application of DTT, indicated no difference due to treatment or time post injection (Fig. 2(C)). Thus, similar to aging, LPS decreased the total and NMDAR-mediated components of synaptic transmission. In contrast to aging, the decrease in the NMDAR component was not due to redox state.

Repeated Exposure of LPS Impaired Hippocampal-Dependent Spatial Memory

Prior to LPS treatment, young ($n = 28$) and older ($n = 9$) animals were pre-tested on the cue discrimination and spatial versions of the water maze task. For the cue discrimination task, there was an effect of training [$F(4,140) = 37.06$, $p < 0.0001$] and an effect of age over the training blocks [$F(1,35) = 7.97$, $p < 0.05$] (Fig. 3a). Post hoc ANOVAs for each block indicated that the age effect was due to young animals swimming less distance to find the platform on block 4 [$F(1,35) = 5.01$, $p < 0.05$] and no difference was observed by the end of training (i.e., block 5). The results indicate that both groups were able to acquire the procedural aspects of the task to about the same extent.

For the spatial discrimination version of the water maze task, there was a training effect [$F(4,140) = 32.43$, $p < 0.0001$] in the absence of and age effect, such that the distance to find the escape platform decreased over the training blocks (Fig. 3b). An ANOVA on the DI scores for the acquisition probe trial indicated no age difference and one-group *t*-tests found that the DI scores were greater than chance for both age groups ($p < 0.05$) (Fig. 3c). Together, the results

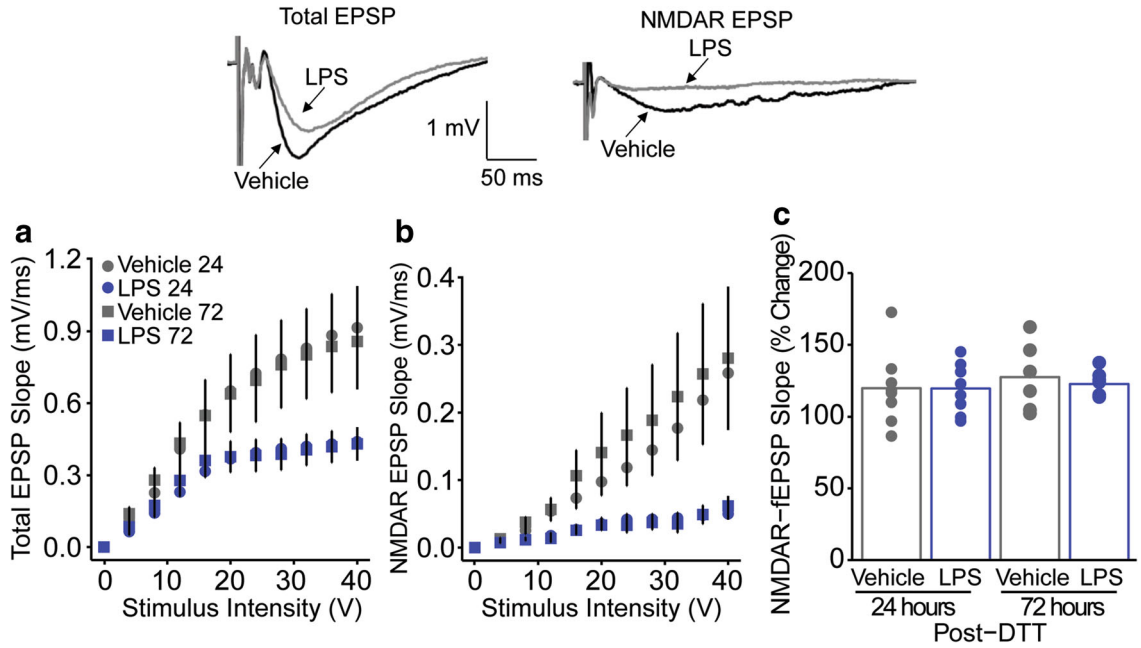

Fig. 2 LPS treatment decreases total and NMDA receptor–mediated synaptic responses in the hippocampus in young LPS animals. Input-output curves for the mean slope (± SEM) of the total fEPSP (A) and NMDA receptor fEPSP (B) evoked by increasing stimulation voltage (V). Data is presented for the vehicle (gray) and LPS treatment (blue) recorded 24 (circles) or 72 (squares) hours after the final injection. (C) Bars illustrating mean percentage change in NMDAR fEPSP slope induced by bath application of DTT in slices obtained from young LPS- or young vehicle-treated animals. The distribution of individual responses is also depicted

indicate both age groups were able to acquire a spatial search strategy to a similar extent.

After pre-testing, young animals were divided into vehicle ($n = 13$) and LPS ($n = 15$) treatment groups. All older animals ($n = 9$) received vehicle injections. Cognitive function was again assessed on the spatial discrimination task 72 h following 6 weeks of LPS or vehicle treatment. A repeated measures ANOVA for swim speed across training blocks indicated no significant group difference (Fig. 4a), confirming an absence of LPS-induced malaise. A repeated measures ANOVA across spatial training blocks on the escape path length indicated a significant main effect of training [$F(4,136) = 17.46$, $p < 0.0001$] and a significant group × training interaction [$F(8,136) = 2.06$, $p < 0.05$] (Fig. 4b). Post hoc analysis found that the interaction between training and group was due to an increased distance for old vehicle animals compared with young vehicle ($p < 0.05$). ANOVAs performed within each training block found a group × training interaction on block 5 [$F(2,34) = 9.05$, $p < 0.01$)] in which young vehicle animals swam a shorter distance to the platform compared with old vehicle.

An ANOVA for the acquisition probe DI scores indicated a significant effect of group [$F(2,34) = 3.43$, $p < 0.05$] (Fig. 4c). Post hoc analysis found that old vehicle animals performed poorly compared with young vehicle ($p < 0.05$). Further, *t*-tests comparing the DI scores relative to chance (i.e., a DI

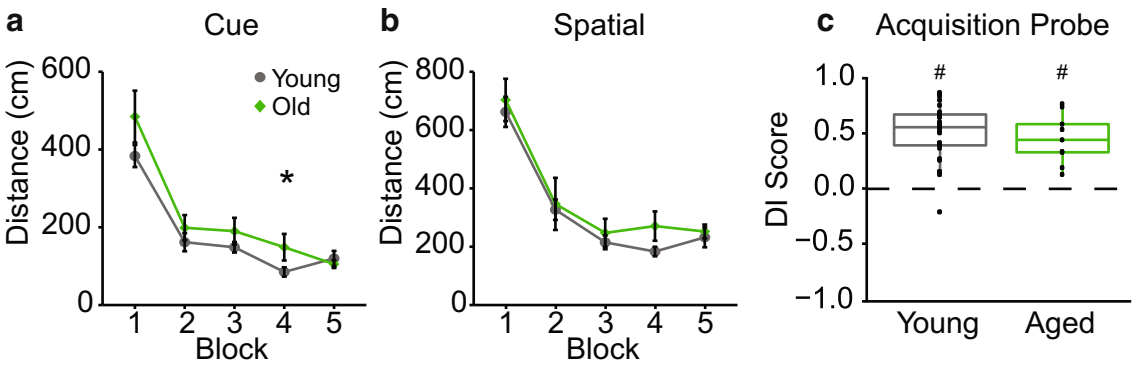

Fig. 3 Minimal age differences in water maze behavior prior to LPS treatment. Symbols represent mean escape path length (± SEM) for young (young gray circle) and middle-age (green diamond) animals over the training blocks for **a** cue and **b** spatial discrimination. **c** Box and whisker plots and individual DI scores from the acquisition probe trial. Asterisk indicates significant difference between groups ($p < 0.05$). Pound sign indicates a significant difference from chance ($p < 0.05$)

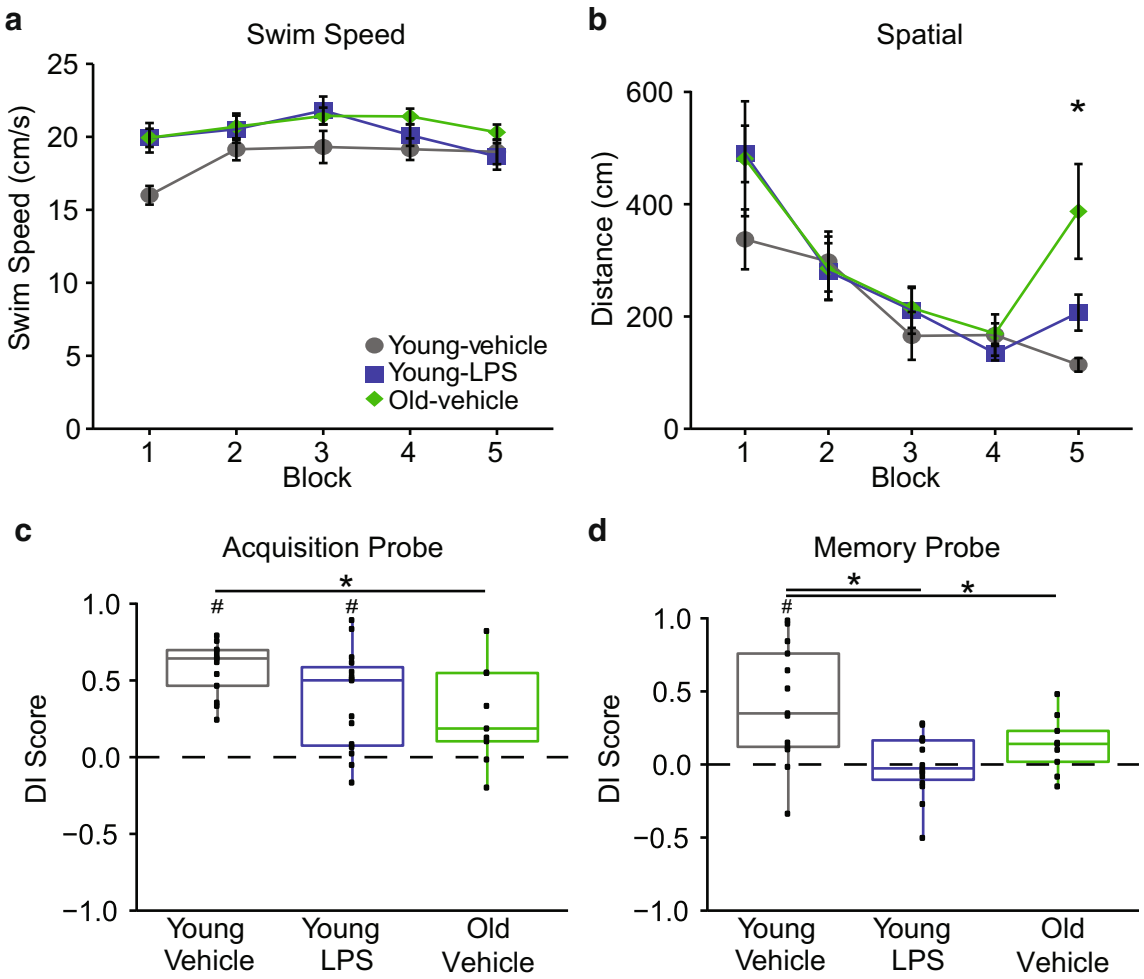

Fig. 4 LPS is associated with impaired episodic spatial memory. Symbols represent mean (± SEM) for **a** swim speed and **b** escape path length over training blocks for young vehicle (gray circle), young LPS (blue square), and older (green diamond) animals. Box and whisker plots and individual points for DI scores from the **c** acquisition and **d** 2-h memory probe trials. Asterisk indicates significant difference ($p < 0.05$) relative to young vehicle. Pound sign indicates a significant difference ($p < 0.05$) from chance

score of 0) for each group indicated that only young vehicle and young LPS exhibited DI scores above chance ($p < 0.05$). For the 2-h memory probe trial, a significant difference was observed across groups [$F(2,34) = 7.34$, $p < 0.01$], due to the superior performance of young vehicle animals relative to young LPS ($p < 0.001$) and old vehicle ($p < 0.05$) (Fig. 4d). In addition, only young vehicle animals exhibited retention DI scores significantly above chance.

The Effect of Systemic Inflammation on Network Connectivity

Functional network connectivity was examined 4 h after the final LPS injection in a subset of young vehicle ($n = 8$) and young LPS ($n = 8$) animals. This time point was selected because previous research indicates that cytokine levels in the blood peak ~4 h after an LPS injection [37]. Significant interactions were observed between treatment × small world coefficient [$F(8,112) = 5.99$, $p < 0.0001$] and treatment × path length [$F(8,112) = 4.524$, $p < 0.0001$] over several density threshold levels (Fig. 5a). Young LPS animals exhibited a decline in small world coefficient [density levels: 2 ($p < 0.05$), 5 ($p < 0.05$), 10 ($p < 0.05$)] and an increase in path length [density level 2 ($p < 0.05$)] compared with young vehicle, suggesting a less efficient network in young LPS animals. There was no significant interaction between treatment × clustering coefficient over the different density levels (Fig. 5a). The overall reduction in connectivity strength after systemic inflammation can also be observed in connectomic maps (Fig. 5b).

Next, an ROI specific analysis was performed in which functional connectivity with a particular seed region was assessed (Fig. 5c–e). Interestingly, there was no change in the functional connectivity within the hippocampus after LPS treatment. We did observe a decrease in functional connectivity with the retrosplenial cortex (RSC), which has reciprocal connections with the hippocampus and plays a role in episodic memory and navigation [38]. Seed-based analysis

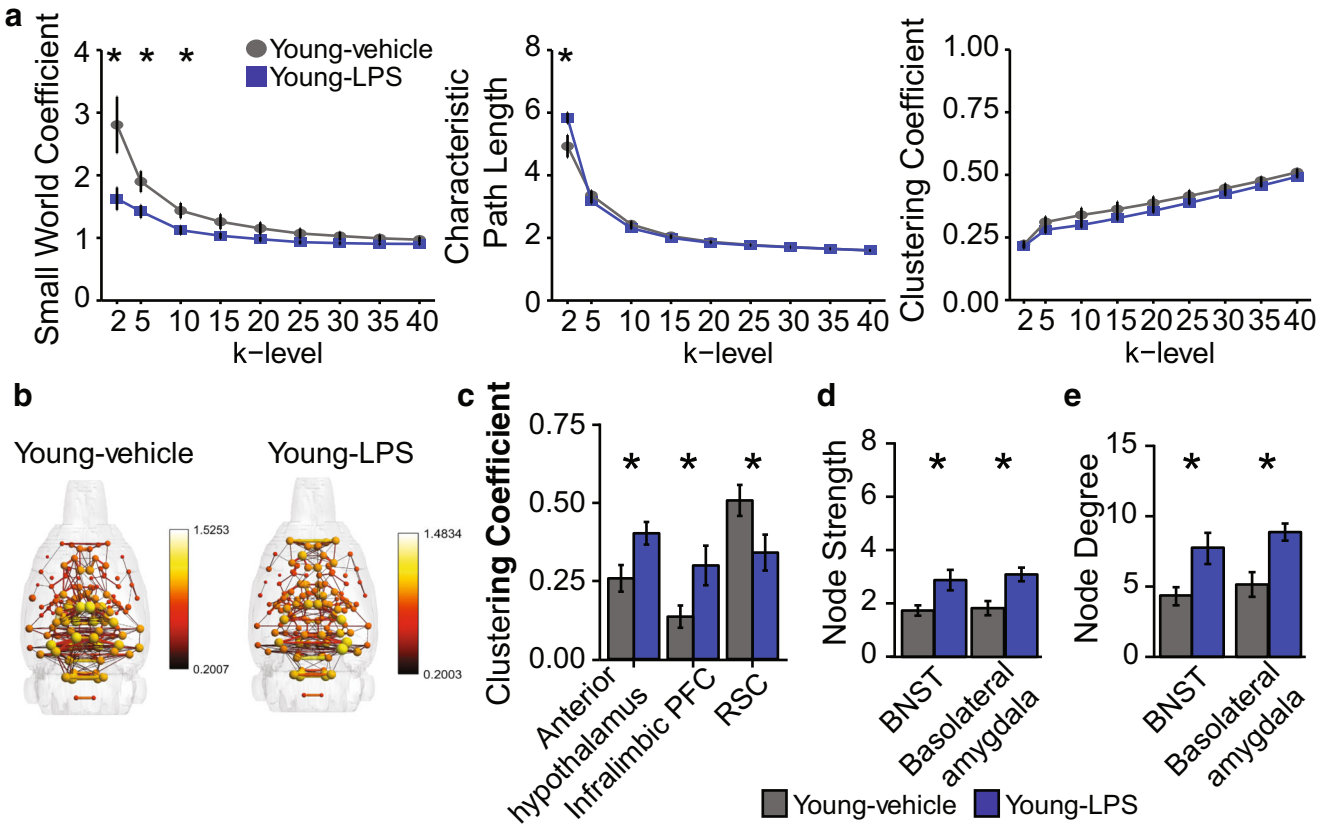

Fig. 5 Reduced global network connectivity was observed 4 h after the last LPS treatment. **a** Symbols represent mean (± SEM) for small world coefficient (left), path length (center), and clustering coefficient (right) over the different *k* levels (graph density thresholds) for young vehicle (gray circle) and young LPS (blue square) animals. **b** Three-dimensional functional connectivity maps of the rat brain illustrating a reduction of connectivity in young LPS-treated ($n = 8$) animals compared with young vehicle ($n = 8$). The size of the sphere represents node strength and the thickness of the line represents edge weights. **c**–**e** Bars represent mean (± SEM) for clustering coefficient (**c**), node strength (**d**), and node degree (**e**) for ROIs that exhibit a significant effect of treatment. Asterisks indicate significant difference between groups ($p < 0.05$). (RSC, retrosplenial cortex; BNST, bed nucleus of the stria terminalis)

found an increase in functional coupling between the RSC and basolateral amygdala (Supplementary Fig. 2). In addition, areas associated with anxiety, fear response, and regulation of body temperature (bed nucleus of the stria terminalis (BNST), infralimbic prefrontal cortex, and anterior hypothalamus) exhibited an increase in functional activity.

The Effect of Systemic Inflammation on Synaptic Proteins

To determine if repeated injections of LPS decreased synaptic protein levels, Western blots were performed on the hippocampus from a subset of behaviorally characterized young animals (young LPS: $n = 6$; young vehicle: $n = 5$–6). The pre-synaptic marker, synaptophysin, and the post-synaptic marker, PSD-95, were both analyzed to determine if either side of the synapse was altered after 48 h after the last LPS injection. Since there was an observed decrease in the synaptic response of the NMDAR in the electrophysiological data, Western blots were also performed on the GluN1 subunit of the NMDAR. However, no effect of LPS treatment on the concentration of the pre-synaptic marker synaptophysin or in the post-synaptic markers PSD-95 and GluN1 was observed (Fig. 6).

The Effect of Systemic Inflammation and Age on the Transcriptome

RNA sequencing was performed on the CA1 and DG regions of the hippocampus 48 h after the last injection, from a subset of behaviorally characterized young (young LPS: $n = 8$; young vehicle: $n = 8$) and older ($n = 6$) animals. Differential expression analyses were performed to specifically examine the effect of age (older vehicle compared with young vehicle) and the effect of LPS treatment (young LPS compared with young vehicle).

CA1

The effect of age on transcription was examined by determining the number of genes that were differentially expressed between old vehicle and young vehicle. There were 894 genes that increased and 386 that decreased expression in old vehicle

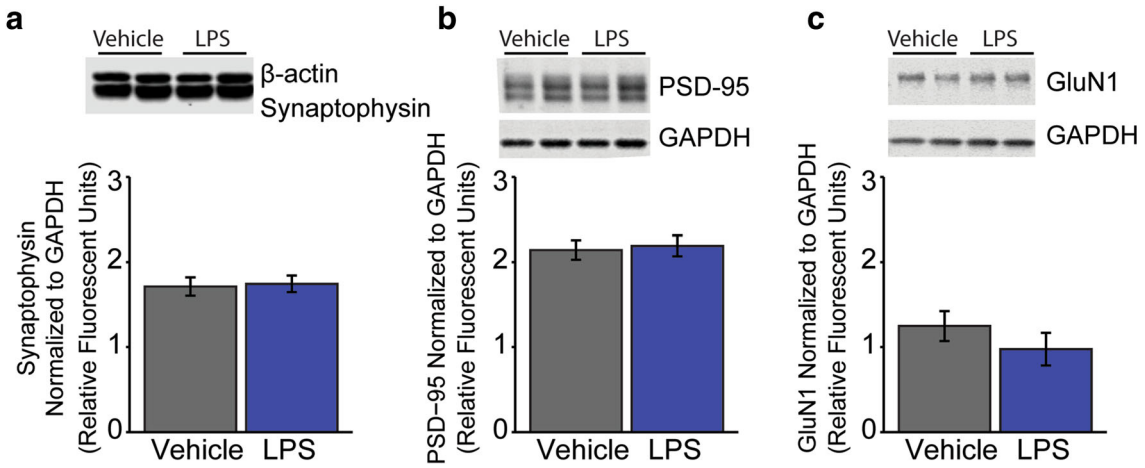

Fig. 6 LPS treatment did not alter synaptic protein levels. Western blots quantifying synaptic proteins in the hippocampus from young animals injected with either vehicle or LPS. The bars represent the means (± SEM) for the expression of the synaptic proteins synaptophysin (**a**), PSD-95 (**b**), and GluN1 (**c**)

compared with young vehicle animals. Similar to numerous studies that report age-related changes in the transcriptome, genes related to inflammatory response and oxidation-reduction process increased with age (Fig. 7a). Further, genes related to neural function, including GO terms for synapse, dendrite, and modulation of synaptic transmission, were downregulated with age (Fig. 7a). When analyzing the effect of treatment, 332 genes were upregulated and 202 genes were downregulated in the young LPS animals compared with young vehicle. Surprisingly, functional annotation analysis found that genes that were increased with LPS treatment cluster for the GO term synapse, which was a GO term noted to decrease with age (Fig. 7a). Indeed, many genes related to neural function were increased 48 h after LPS treatment,

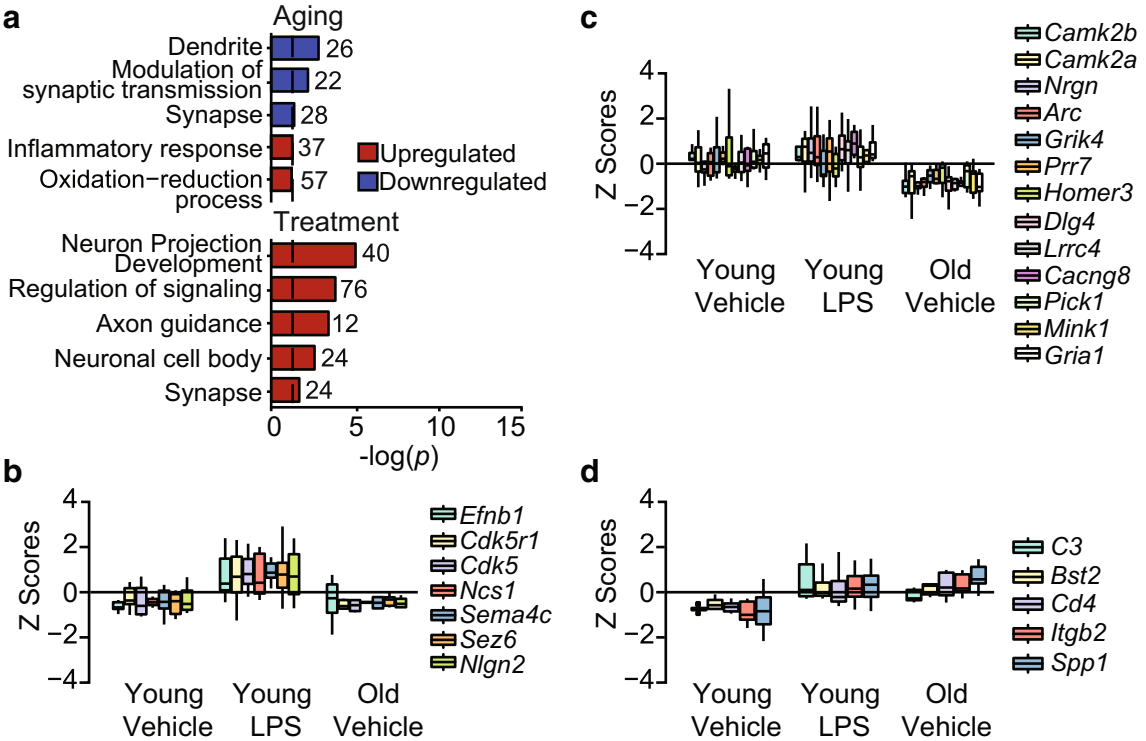

Fig. 7 Differential expression analysis evaluating the effect of age or treatment in the CA1 region. **a** Bars represent the –log(*p* value) for selected GO terms that were significant from the two different analyses performed: (1) Aging: old vehicle v young vehicle and (2) Treatment: young LPS v young vehicle. Dotted line is the –log(0.05). GO terms are split by direction of change (upregulated red; downregulated blue). The number to the right of each bar represents the number of genes that were found in that GO term. **b**, **c** Boxplots of genes that were within the GO term synapse that were altered with treatment (**b**) or age (**c**). **d** Boxplots of inflammatory genes that were increased with both age and LPS treatment

including genes linked to the GO terms neuron projection development, regulation of signaling, axon guidance, neuronal cell body, and synapse (Fig. 7a). Next, we examined similarities or differences between the effect of LPS treatment and age on the hippocampal transcriptome. First, we analyzed the genes within the GO term synapse because this GO term was dysregulated with both age and LPS treatment. It is interesting to note that synapse genes that decreased with age were not the same synapse genes that increased with treatment (Supplementary Table 2). For treatment, genes within the GO term synapse were related to the maintenance and development of dendritic spines or axons (*Efnb1*, *Cdk5r1*, *Cdk5*, *Ncs1*, *Sema4c*, *Sez6, Nlgn2*) (Fig. 7b). In contrast, aging was associated with a decrease in genes related to mechanisms of synaptic plasticity (*Camk2b*, *Camk2a*, *Nrgn*, *Crtc1, Arc*) or post-synaptic receptors/scaffold proteins (*Grik4*, *Prr7*, *Homer3*, *Dlg4*, *Lrrc4*, *Cacng8*, *Pick1*, *Mink1*, *Gria1*, *Grasp*) (Fig. 7c). Finally, we compared genes that were changed in the same direction when comparing either old vehicle or young LPS with young vehicle. There were 16 genes that increased and 11 genes that decreased with both age and LPS treatment. When analyzing the genes that increased across both analyses, these genes were related to inflammation, including *C3*, *Bst2*, *Cd4*, *Itgb2*, and *Spp1* (Fig. 7d).

DG

When comparing old vehicle with young vehicle, there were fewer number of differentially expressed genes (DEGs) in the DG compared with the CA1, with 77 genes that increased and 135 genes that decreased expression. Similar to the CA1, the GO term inflammatory response was observed to increase with age (Supplementary Fig. 3A). In addition, several distinct GO terms were clustered for upregulated genes, including lysosome, oxygen-containing compound, and the KEGG pathway phagosome (Supplementary Fig. 3A). Analyzing the effect of LPS treatment on DG gene expression yielded 313 genes that were upregulated and 310 genes that were downregulated in young LPS animals compared with young vehicle. In contrast to the CA1, there was no change in genes related to synaptic function. Instead, functional annotation analysis indicated that upregulated genes were related to RNA splicing, gene expression, and nuclear body (Supplementary Fig. 3A). Genes that were downregulated in the young LPS compared with young vehicle were related to peptide metabolic process and extracellular exosome (Supplementary Fig. 3A). Only a few genes were similarly dysregulated when comparing old vehicle or young LPS with young vehicle. A total of 16 genes were increased and 10 genes were decreased across both analyses. Similar to CA1, genes that increased in old vehicle and young LPS compared with young vehicle were related to inflammation (*C3*, *Fcgr2b*, *Dlx1*) (Supplementary Fig. 3B).

Discussion

Systemic inflammation in older individuals correlates with cognitive deficits [39, 40] and systemic inflammation in adults can predict cognitive decline examined up to 20 years later [4, 5]. However, the mechanism linking peripheral inflammation to brain aging and age-related cognitive impairment is not clear. Acute administration of LPS has often been employed to examine the possible mechanisms through which systemic inflammation can disrupt cognition. Potential mechanisms include elevated cytokine levels, increased oxidative stress, activation of glial cells, and impaired synaptic function. Interestingly, the literature suggests that acute LPS treatment induces a sequential and time-limited activation of these possible mechanisms, which may differentially influence learning and memory. However, it is unclear whether peripheral inflammation induces long-term changes associated with brain aging.

Effects of Repeated LPS Treatment in Young Animals In young animals, LPS treatment impaired memory 72 h after the last injection in the absence of altered acquisition of spatial information. Previous research indicates that impaired learning is observed 2–24 h after LPS injections [41–44]. However, this time period is also associated with malaise, which can confound performance on cognitive tasks [45]. The effect of LPS on our behavioral results is not likely due to sickness, since sickness behavior usually resolves as plasma cytokine levels return to baseline, usually within 24 h after an injection [37, 46]. In addition, we observed no rise in temperature after the sixth injection and an initial weight loss was limited to weeks 1–2 after the initiation of LPS treatments, consistent with decreased cytokine release due to endotoxin tolerance [35]. Finally, repeated LPS treatment did not cause a slower swim speed, supporting the absence of malaise at the time of testing.

Systemic Inflammation as a Mechanism for Senescence A goal of the current study was to determine if repeated LPS injections mimic aging. A reduction in global network connectivity was observed 4 h after the final injection. It is unclear whether the reduction in connectivity was due to long-term effects associated with the initial LPS injection, repeated LPS injections, or an acute effect due to the last LPS injection. However, it should be noted that a reduction in global network connectivity has been reported for systemic inflammation [47, 48] and aging [49–51].

The LPS-induced memory deficits, increase in inflammatory genes, and decrease in synaptic transmission are similar to impaired consolidation of episodic spatial memory, transcriptional profile changes, and altered synaptic transmission observed during aging [33, 52, 53]. While the observed results may be due to long-term effects of the initial injection,

previous research indicates no cognitive deficits 7 weeks after an acute LPS injection [54]. Together, the results suggest that repeated LPS injections continue to influence cognition and the brain, despite reduced cytokine release associated with tolerance [55–57].

Altered hippocampal synaptic function provides one of the primary electrophysiological markers for the emergence of memory deficits, starting in middle age [36, 52, 58], including a redox-mediated decline in NMDAR function [10]. Similar to aging, LPS decreased the total and NMDAR-mediated components of synaptic transmission, consistent with the idea that impaired hippocampal synaptic function contributes to delay-dependent memory deficits [52, 58]. However, the decrease in the NMDAR response was not redox sensitive, suggesting that the decrease in synaptic function following LPS treatment may be different from aging. Alternatively, we may have missed early redox changes associated with direct effects of cytokines. Production of reactive oxygen species by LPS and cytokines occurs within minutes [59–62]. In turn, reactive oxygen species impairs synaptic function and promotes synaptic loss [43, 63–65]. In the case of LPS injections, cytokines return to baseline levels hours after an injection of LPS [37, 46]. In contrast, aging is associated with chronic systemic inflammation [66]. Interestingly, anti-inflammatory treatments appear to ameliorate the redox-mediated decrease in NMDAR function, suggesting a role for ongoing inflammation during aging in the redox regulation of NMDAR function [67].

We found that protein levels of the pre-synaptic marker (synaptophysin) and post-synaptic markers (PSD-95 and GluN1) were not affected 48 h after the last injection. Synaptic protein may decline in the oldest animals; however, changes in hippocampal synaptic proteins between young adult and middle-age are quite variable and protein expression is not necessarily associated with cognitive function [68–72]. Furthermore, the effect of anti-inflammatory treatments on NMDAR expression in aged animals is unclear [73–75]. For LPS treatments, expressions of synaptic marker proteins decrease soon after treatment; however, several reports suggest that, for younger animals, there is no loss of synaptophysin, and recovery of other synaptic proteins is observed within days following treatment [76–79]. Together, the results indicate that LPS treatment does not completely recapitulate the aging phenotype for synaptic function, possibly due to the chronic nature of systemic inflammation in aging and resilience of young animals to acute treatments.

Resilience Mechanisms of Young Animals Young animals exhibit cognitive impairments and elevated neuroinflammation immediately after a week of daily LPS injections (5–10 mg/kg), but the effects of the 5 mg LPS treatment resolved within 30 days [80]. Indeed, we have observed that weekly treatment of young animals (1 mg/kg) did not impair memory months later (Supplementary Fig. 4). Similarly, an LPS-induced impairment in synaptic function [81] and loss of synaptic proteins [82] recovered a week after cessation of LPS treatment. It is possible that recovery involved altered gene expression similar to that observed in the current study. Young LPS animals exhibit an increase in expression of synaptic genes, including an increase in the gene for PSD-95 (*Dlg4*). The idea of transcriptional resilience of synaptic genes in young animals is consistent with the time course of hippocampal gene expression following systemic inflammation induced by sepsis [83]. Young mice exhibit decreased neuronal and synaptic genes in the hippocampus, 24 h after the initiation of sepsis, which recovered over 4 days. In contrast, for old male mice, neuronal and synaptic genes continued to decrease and immune response genes continued to increase on day 4 of sepsis. The researchers suggested that the resilience or vulnerability to systemic inflammation may depend on the pre-existing inflammatory state [83]. Consistent with previous work, older animals exhibited increased expression of immune response genes and decreased expression of synaptic and synaptic plasticity genes [33, 34, 83]. In addition, we observed increased expression genes linked to synapse elimination (*Mertk*, *Megf10*) [84]. Thus, we would suggest that increased expression of genes for growth and maintenance of synapses in young animals represents neuronal resilience/recovery in response to acute systemic inflammation and the decrease in synaptic function and the age-related decrease in expression of synaptic genes may depend on ongoing chronic inflammation.

It appears that, while LPS induces some changes similar to those seen with aging, the LPS treatment parameters employed in the current study do not completely recapitulate the aging phenotype, possibly due to the acute versus chronic nature of the inflammation. At this point, we can only speculate as to how systemic inflammation might drive brain aging and cognitive decline. The current study suggests that systemic inflammation during aging could contribute to a decrease in synaptic transmission, increased transcription of immune response genes, and impaired memory. The increase in microglial and inflammation-related genes may result in tolerance or priming of the brain's response to the low-level chronic systemic inflammation of aging. Finally, an increase in inflammation signaling and decrease in synaptic signaling could influence epigenetic regulation of neuroinflammatory and synaptic gene transcription [85].

Conclusion

In young animals, repeated exposure of LPS induces several characteristics of aging, such as impaired hippocampal synaptic transmission, cognitive decline, and increased expression of immune responsive genes. However, despite this decline in hippocampal function, young animals exhibited upregulation of genes that maintain synaptic function, which may permit recovery of hippocampal function. Finally, inflammation in

adulthood may act through epigenetic mechanisms or microglial priming to sensitize the brain to low-level systemic inflammation observed during aging.

Acknowledgments Special thanks to Nick Sarantos, Sophia Eikenberry, and Valentina Lavieri-Sosa for their assistance in animal handling and behavior assessment.

Funding Information This study was financially supported by the National Institute of Aging grants R01AG037984, R37AG036800, R01049711, and R01052258 and the Evelyn F. McKnight Brain Research Foundation. This work was partially supported by the University of Florida Claude D Pepper Older American Independence Center (P30-AG028740). Authors also received financial support from the National High Magnetic Field Laboratory's Advanced Magnetic Resonance Imaging & Spectroscopy (AMRIS) Facility (National Science Foundation Cooperative Agreement No. DMR-1157490 and the State of Florida).

Compliance with Ethical Standards

All procedures involving animals were approved by the Institutional Animal Care and Use Committee at the University of Florida and were in agreement with guidelines recognized by the U.S. Public Health Service Policy on Humane Care and Use of Laboratory Animals.

Conflict of Interest The authors declare that they have no competing interests.

References

1. Ventura MT, Casciaro M, Gangemi S, Buquicchio R (2017) Immunosenescence in aging: between immune cells depletion and cytokines up-regulation. Clin Mol Allergy 15:21. https://doi.org/10.1186/s12948-017-0077-0
2. Mariani E, Cattini L, Neri S, Malavolta M, Mocchegiani E, Ravaglia G, Facchini A (2006) Simultaneous evaluation of circulating chemokine and cytokine profiles in elderly subjects by multiplex technology: relationship with zinc status. Biogerontology 7(5–6):449–459. https://doi.org/10.1007/s10522-006-9060-8
3. Wei J, Xu H, Davies JL, Hemmings GP (1992) Increase of plasma IL-6 concentration with age in healthy subjects. Life Sci 51(25):1953–1956. https://doi.org/10.1016/0024-3205(92)90112-3
4. Walker KA, Gottesman RF, Wu A, Knopman DS, Gross AL, Mosley TH Jr, Selvin E, Windham BG (2019) Systemic inflammation during midlife and cognitive change over 20 years: the ARIC study. Neurology 92(11):e1256–e1267. https://doi.org/10.1212/WNL.0000000000007094
5. Beydoun MA, Dore GA, Canas JA, Liang H, Beydoun HA, Evans MK, Zonderman AB (2018) Systemic inflammation is associated with longitudinal changes in cognitive performance among urban adults. Front Aging Neurosci 10:313. https://doi.org/10.3389/fnagi.2018.00313
6. Streit WJ, Xue QS, Tischer J, Bechmann I (2014) Microglial pathology. Acta Neuropathol Commun 2:142. https://doi.org/10.1186/s40478-014-0142-6
7. Barrientos RM, Kitt MM, Watkins LR, Maier SF (2015) Neuroinflammation in the normal aging hippocampus. Neuroscience 309:84–99. https://doi.org/10.1016/j.neuroscience.2015.03.007
8. Cakatay U, Telci A, Kayali R, Tekeli F, Akcay T, Sivas A (2001) Relation of oxidative protein damage and nitrotyrosine levels in the aging rat brain. Exp Gerontol 36(2):221–229
9. Kumar A, Yegla B, Foster TC (2018) Redox signaling in neurotransmission and cognition during aging. Antioxid Redox Signal 28(18):1724–1745. https://doi.org/10.1089/ars.2017.7111
10. Kumar A, Foster TC (2013) Linking redox regulation of NMDAR synaptic function to cognitive decline during aging. J Neurosci 33(40):15710–15715. https://doi.org/10.1523/JNEUROSCI.2176-13.2013
11. Barnes CA, Rao G, Shen J (1997) Age-related decrease in the N-methyl-D-aspartateR-mediated excitatory postsynaptic potential in hippocampal region CA1. Neurobiol Aging 18(4):445–452
12. Banks WA, Robinson SM (2010) Minimal penetration of lipopolysaccharide across the murine blood-brain barrier. Brain Behav Immun 24(1):102–109. https://doi.org/10.1016/j.bbi.2009.09.001
13. Yirmiya R, Goshen I (2011) Immune modulation of learning, memory, neural plasticity and neurogenesis. Brain Behav Immun 25(2):181–213. https://doi.org/10.1016/j.bbi.2010.10.015
14. Bodhinathan K, Kumar A, Foster TC (2010) Intracellular redox state alters NMDA receptor response during aging through Ca2+/calmodulin-dependent protein kinase II. J Neurosci 30(5):1914–1924. https://doi.org/10.1523/JNEUROSCI.5485-09.2010
15. Kumar A, Rani A, Tchigranova O, Lee WH, Foster TC (2012) Influence of late-life exposure to environmental enrichment or exercise on hippocampal function and CA1 senescent physiology. Neurobiol Aging 33(4):828 e821–828 e817. https://doi.org/10.1016/j.neurobiolaging.2011.06.023
16. Kumar A, Thinschmidt JS, Foster TC (2019) Subunit contribution to NMDA receptor hypofunction and redox sensitivity of hippocampal synaptic transmission during aging. k 11(14):5140–5157. https://doi.org/10.18632/aging.102108
17. Bean LA, Kumar A, Rani A, Guidi M, Rosario AM, Cruz PE, Golde TE, Foster TC (2015) Re-opening the critical window for estrogen therapy. J Neurosci 35(49):16077–16093. https://doi.org/10.1523/JNEUROSCI.1890-15.2015
18. Guidi M, Kumar A, Rani A, Foster TC (2014) Assessing the emergence and reliability of cognitive decline over the life span in Fisher 344 rats using the spatial water maze. Front Aging Neurosci 6:2. https://doi.org/10.3389/fnagi.2014.00002
19. LaClair M, Febo M, Nephew B, Gervais NJ, Poirier G, Workman K, Chumachenko S, Payne L et al (2019) Sex differences in cognitive flexibility and resting brain networks in middle-aged marmosets. eNeuro 6(4):ENEURO.0154–ENEU19.2019. https://doi.org/10.1523/ENEURO.0154-19.2019
20. Orsini CA, Colon-Perez LM, Heshmati SC, Setlow B, Febo M (2018) Functional connectivity of chronic cocaine use reveals progressive neuroadaptations in neocortical, striatal, and limbic networks. eNeuro 5(4):ENEURO.0081–ENEU18.2018. https://doi.org/10.1523/ENEURO.0081-18.2018
21. Colon-Perez LM, Tran K, Thompson K, Pace MC, Blum K, Goldberger BA, Gold MS, Bruijnzeel AW et al (2016) The psychoactive designer drug and Bath salt constituent MDPV causes widespread disruption of brain functional connectivity. Neuropsychopharmacology 41(9):2352–2365. https://doi.org/10.1038/npp.2016.40
22. Jenkinson M, Bannister P, Brady M, Smith S (2002) Improved optimization for the robust and accurate linear registration and motion correction of brain images. Neuroimage 17(2):825–841
23. Cox RW (1996) AFNI: Software for analysis and visualization of functional magnetic resonance neuroimages. Comput Biomed Res 29(3):162–173
24. Rubinov M, Sporns O (2010) Complex network measures of brain connectivity: uses and interpretations. Neuroimage 52(3):1059–1069. https://doi.org/10.1016/j.neuroimage.2009.10.003

25. Newman ME, Girvan M (2004) Finding and evaluating community structure in networks. Phys Rev E Stat Nonlinear Soft Matter Phys 69(2 Pt 2):026113. https://doi.org/10.1103/PhysRevE.69.026113
26. Newman MEJ (2003) The structure and function of complex networks. SIAM Rev 45(2):167–256. https://doi.org/10.1137/S003614450342480
27. Boccaletti S, Latora V, Moreno Y, Chavez M, Hwang DU (2006) Complex networks: structure and dynamics. Phys Rep 424(4–5):175–308. https://doi.org/10.1016/j.physrep.2005.10.009
28. Saramaki J, Kivela M, Onnela JP, Kaski K, Kertesz J (2007) Generalizations of the clustering coefficient to weighted complex networks. Phys Rev E Stat Nonlinear Soft Matter Phys 75(2 Pt 2):027105. https://doi.org/10.1103/PhysRevE.75.027105
29. Humphries MD, Gurney K (2008) Network 'small-world-ness': a quantitative method for determining canonical network equivalence. PLoS One 3(4):e0002051. https://doi.org/10.1371/journal.pone.0002051
30. Watts DJ, Strogatz SH (1998) Collective dynamics of 'small-world' networks. Nature 393(6684):440–442. https://doi.org/10.1038/30918
31. Newman ME (2018) Networks: an introduction, 2nd Edition. Oxford University Press, Oxford, England.
32. Han X, Aenlle KK, Bean LA, Rani A, Semple-Rowland SL, Kumar A, Foster TC (2013) Role of estrogen receptor alpha and beta in preserving hippocampal function during aging. J Neurosci 33(6):2671–2683. https://doi.org/10.1523/JNEUROSCI.4937-12.2013
33. Ianov L, De Both M, Chawla MK, Rani A, Kennedy AJ, Piras I, Day JJ, Siniard A et al (2017) Hippocampal transcriptomic profiles: subfield vulnerability to age and cognitive impairment. Front Aging Neurosci 9:383. https://doi.org/10.3389/fnagi.2017.00383
34. Ianov L, Rani A, Beas BS, Kumar A, Foster TC (2016) Transcription profile of aging and cognition-related genes in the medial prefrontal cortex. Front Aging Neurosci 8:113. https://doi.org/10.3389/fnagi.2016.00113
35. Zeisberger E, Roth J (1998) Tolerance to pyrogens. Ann N Y Acad Sci 856:116–131. https://doi.org/10.1111/j.1749-6632.1998.tb08320.x
36. Foster TC (2019) Senescent neurophysiology: Ca(2+) signaling from the membrane to the nucleus. Neurobiol Learn Mem 164:107064. https://doi.org/10.1016/j.nlm.2019.107064
37. Erickson MA, Banks WA (2011) Cytokine and chemokine responses in serum and brain after single and repeated injections of lipopolysaccharide: multiplex quantification with path analysis. Brain Behav Immun 25(8):1637–1648. https://doi.org/10.1016/j.bbi.2011.06.006
38. Vann SD, Aggleton JP, Maguire EA (2009) What does the retrosplenial cortex do? Nat Rev Neurosci 10(11):792–802. https://doi.org/10.1038/nrn2733
39. Schram MT, Euser SM, de Craen AJ, Witteman JC, Frolich M, Hofman A, Jolles J, Breteler MM et al (2007) Systemic markers of inflammation and cognitive decline in old age. J Am Geriatr Soc 55(5):708–716. https://doi.org/10.1111/j.1532-5415.2007.01159.x
40. Bourassa K, Sbarra DA (2017) Body mass and cognitive decline are indirectly associated via inflammation among aging adults. Brain Behav Immun 60:63–70. https://doi.org/10.1016/j.bbi.2016.09.023
41. Arai K, Matsuki N, Ikegaya Y, Nishiyama N (2001) Deterioration of spatial learning performances in lipopolysaccharide-treated mice. Jpn J Pharmacol 87(3):195–201
42. Badshah H, Ali T, Kim MO (2016) Osmotin attenuates LPS-induced neuroinflammation and memory impairments via the TLR4/NFkappaB signaling pathway. Sci Rep 6:24493. https://doi.org/10.1038/srep24493
43. Anaeigoudari A, Soukhtanloo M, Shafei MN, Sadeghnia HR, Reisi P, Beheshti F, Behradnia S, Mousavi SM et al (2016) Neuronal nitric oxide synthase has a role in the detrimental effects of lipopolysaccharide on spatial memory and synaptic plasticity in rats. Pharmacol Rep 68(2):243–249. https://doi.org/10.1016/j.pharep.2015.09.004
44. Gao J, Xiong B, Zhang B, Li S, Huang N, Zhan G, Jiang R, Yang L et al (2018) Sulforaphane alleviates lipopolysaccharide-induced spatial learning and memory dysfunction in mice: the role of BDNF-mTOR signaling pathway. Neuroscience 388:357–366. https://doi.org/10.1016/j.neuroscience.2018.07.052
45. Cunningham C, Sanderson DJ (2008) Malaise in the water maze: untangling the effects of LPS and IL-1beta on learning and memory. Brain Behav Immun 22(8):1117–1127. https://doi.org/10.1016/j.bbi.2008.05.007
46. Norden DM, Trojanowski PJ, Villanueva E, Navarro E, Godbout JP (2016) Sequential activation of microglia and astrocyte cytokine expression precedes increased Iba-1 or GFAP immunoreactivity following systemic immune challenge. Glia 64(2):300–316. https://doi.org/10.1002/glia.22930
47. Dipasquale O, Cooper EA, Tibble J, Voon V, Baglio F, Baselli G, Cercignani M, Harrison NA (2016) Interferon-alpha acutely impairs whole-brain functional connectivity network architecture - a preliminary study. Brain Behav Immun 58:31–39. https://doi.org/10.1016/j.bbi.2015.12.011
48. Labrenz F, Wrede K, Forsting M, Engler H, Schedlowski M, Elsenbruch S, Benson S (2016) Alterations in functional connectivity of resting state networks during experimental endotoxemia - an exploratory study in healthy men. Brain Behav Immun 54:17–26. https://doi.org/10.1016/j.bbi.2015.11.010
49. Onoda K, Ishihara M, Yamaguchi S (2012) Decreased functional connectivity by aging is associated with cognitive decline. J Cogn Neurosci 24(11):2186–2198. https://doi.org/10.1162/jocn_a_00269
50. Geerligs L, Renken RJ, Saliasi E, Maurits NM, Lorist MM (2015) A brain-wide study of age-related changes in functional connectivity. Cereb Cortex 25(7):1987–1999. https://doi.org/10.1093/cercor/bhu012
51. Varangis E, Razlighi Q, Habeck CG, Fisher Z, Stern Y (2019) Between-network functional connectivity is modified by age and cognitive task domain. J Cogn Neurosci 31(4):607–622. https://doi.org/10.1162/jocn_a_01368
52. Foster TC (2012) Dissecting the age-related decline on spatial learning and memory tasks in rodent models: N-methyl-D-aspartate receptors and voltage-dependent Ca2+ channels in senescent synaptic plasticity. Prog Neurobiol 96(3):283–303. https://doi.org/10.1016/j.pneurobio.2012.01.007
53. Masser DR, Bixler GV, Brucklacher RM, Yan H, Giles CB, Wren JD, Sonntag WE, Freeman WM (2014) Hippocampal subregions exhibit both distinct and shared transcriptomic responses to aging and nonneurodegenerative cognitive decline. J Gerontol A Biol Sci Med Sci 69(11):1311–1324. https://doi.org/10.1093/gerona/glu091
54. Valero J, Mastrella G, Neiva I, Sanchez S, Malva JO (2014) Long-term effects of an acute and systemic administration of LPS on adult neurogenesis and spatial memory. Front Neurosci 8:83. https://doi.org/10.3389/fnins.2014.00083
55. Kahn MS, Kranjac D, Alonzo CA, Haase JH, Cedillos RO, McLinden KA, Boehm GW, Chumley MJ (2012) Prolonged elevation in hippocampal Abeta and cognitive deficits following repeated endotoxin exposure in the mouse. Behav Brain Res 229(1):176–184. https://doi.org/10.1016/j.bbr.2012.01.010
56. Fischer CW, Elfving B, Lund S, Wegener G (2015) Behavioral and systemic consequences of long-term inflammatory challenge. J Neuroimmunol 288:40–46. https://doi.org/10.1016/j.jneuroim.2015.08.011
57. Yegla B, Foster T (2019) Effect of systemic inflammation on rat attentional function and neuroinflammation: possible protective role for food restriction. Front Aging Neurosci 11:296. https://doi.org/10.3389/fnagi.2019.00296

58. Foster TC (1999) Involvement of hippocampal synaptic plasticity in age-related memory decline. Brain Res Brain Res Rev 30(3): 236–249. https://doi.org/10.1016/s0165-0173(99)00017-x
59. Ishihara Y, Takemoto T, Itoh K, Ishida A, Yamazaki T (2015) Dual role of superoxide dismutase 2 induced in activated microglia: oxidative stress tolerance and convergence of inflammatory responses. J Biol Chem 290(37):22805–22817. https://doi.org/10.1074/jbc.M115.659151
60. Pawate S, Shen Q, Fan F, Bhat NR (2004) Redox regulation of glial inflammatory response to lipopolysaccharide and interferongamma. J Neurosci Res 77(4):540–551. https://doi.org/10.1002/jnr.20180
61. Qin L, Liu Y, Wang T, Wei SJ, Block ML, Wilson B, Liu B, Hong JS (2004) NADPH oxidase mediates lipopolysaccharide-induced neurotoxicity and proinflammatory gene expression in activated microglia. J Biol Chem 279(2):1415–1421. https://doi.org/10.1074/jbc.M307657200
62. Yang D, Elner SG, Bian ZM, Till GO, Petty HR, Elner VM (2007) Pro-inflammatory cytokines increase reactive oxygen species through mitochondria and NADPH oxidase in cultured RPE cells. Exp Eye Res 85(4):462–472. https://doi.org/10.1016/j.exer.2007.06.013
63. Lynch MA (1998) Age-related impairment in long-term potentiation in hippocampus: a role for the cytokine, interleukin-1 beta? Prog Neurobiol 56(5):571–589
64. Sunico CR, Gonzalez-Forero D, Dominguez G, Garcia-Verdugo JM, Moreno-Lopez B (2010) Nitric oxide induces pathological synapse loss by a protein kinase G-, Rho kinase-dependent mechanism preceded by myosin light chain phosphorylation. J Neurosci 30(3):973–984. https://doi.org/10.1523/JNEUROSCI.3911-09.2010
65. Vereker E, O'Donnell E, Lynch A, Kelly A, Nolan Y, Lynch MA (2001) Evidence that interleukin-1beta and reactive oxygen species production play a pivotal role in stress-induced impairment of LTP in the rat dentate gyrus. Eur J Neurosci 14(11):1809–1819. https://doi.org/10.1046/j.0953-816x.2001.01809.x
66. Scheinert RB, Asokan A, Rani A, Kumar A, Foster TC, Ormerod BK (2015) Some hormone, cytokine and chemokine levels that change across lifespan vary by cognitive status in male Fischer 344 rats. Brain Behav Immun 49:216–232. https://doi.org/10.1016/j.bbi.2015.06.005
67. Kumar A, Rani A, Scheinert RB, Ormerod BK, Foster TC (2018) Nonsteroidal anti-inflammatory drug, indomethacin improves spatial memory and NMDA receptor function in aged animals. Neurobiol Aging 70:184–193. https://doi.org/10.1016/j.neurobiolaging.2018.06.026
68. Mladenovic Djordjevic A, Perovic M, Tesic V, Tanic N, Rakic L, Ruzdijic S, Kanazir S (2010) Long-term dietary restriction modulates the level of presynaptic proteins in the cortex and hippocampus of the aging rat. Neurochem Int 56(2):250–255. https://doi.org/10.1016/j.neuint.2009.10.008
69. Nyffeler M, Zhang WN, Feldon J, Knuesel I (2007) Differential expression of PSD proteins in age-related spatial learning impairments. Neurobiol Aging 28(1):143–155. https://doi.org/10.1016/j.neurobiolaging.2005.11.003
70. VanGuilder HD, Farley JA, Yan H, Van Kirk CA, Mitschelen M, Sonntag WE, Freeman WM (2011) Hippocampal dysregulation of synaptic plasticity-associated proteins with age-related cognitive decline. Neurobiol Dis 43(1):201–212. https://doi.org/10.1016/j.nbd.2011.03.012
71. Wang R, Tang Y, Feng B, Ye C, Fang L, Zhang L, Li L (2007) Changes in hippocampal synapses and learning-memory abilities in age-increasing rats and effects of tetrahydroxystilbene glucoside in aged rats. Neuroscience 149(4):739–746. https://doi.org/10.1016/j.neuroscience.2007.07.065
72. Magnusson KR, Brim BL, Das SR (2010) Selective vulnerabilities of N-methyl-D-aspartate (NMDA) receptors during brain aging. Front Aging Neurosci 2:11. https://doi.org/10.3389/fnagi.2010.00011
73. Gemma C, Stellwagen H, Fister M, Coultrap SJ, Mesches MH, Browning MD, Bickford PC (2004) Rosiglitazone improves contextual fear conditioning in aged rats. Neuroreport 15(14):2255–2259. https://doi.org/10.1097/00001756-200410050-00023
74. Marquez Loza A, Elias V, Wong CP, Ho E, Bermudez M, Magnusson KR (2017) Effects of ibuprofen on cognition and NMDA receptor subunit expression across aging. Neuroscience 344:276–292. https://doi.org/10.1016/j.neuroscience.2016.12.041
75. Mesches MH, Gemma C, Veng LM, Allgeier C, Young DA, Browning MD, Bickford PC (2004) Sulindac improves memory and increases NMDA receptor subunits in aged Fischer 344 rats. Neurobiol Aging 25(3):315–324. https://doi.org/10.1016/S0197-4580(03)00116-7
76. Shen X, Sun Y, Wang M, Shu H, Zhu LJ, Yan PY, Zhang JF, Jin X (2018) Chronic N-acetylcysteine treatment alleviates acute lipopolysaccharide-induced working memory deficit through up-regulating caveolin-1 and synaptophysin in mice. Psychopharmacology 235(1):179–191. https://doi.org/10.1007/s00213-017-4762-y
77. Zhang S, Wang X, Ai S, Ouyang W, Le Y, Tong J (2017) Sepsis-induced selective loss of NMDA receptors modulates hippocampal neuropathology in surviving septic mice. PLoS One 12(11): e0188273. https://doi.org/10.1371/journal.pone.0188273
78. Zong MM, Yuan HM, He X, Zhou ZQ, Qiu XD, Yang JJ, Ji MH (2019) Disruption of striatal-enriched protein tyrosine phosphatase signaling might contribute to memory impairment in a mouse model of sepsis-associated encephalopathy. Neurochem Res 44(12): 2832–2842. https://doi.org/10.1007/s11064-019-02905-2
79. Kan MH, Yang T, Fu HQ, Fan L, Wu Y, Terrando N, Wang TL (2016) Pyrrolidine dithiocarbamate prevents neuroinflammation and cognitive dysfunction after endotoxemia in rats. Front Aging Neurosci 8:175. https://doi.org/10.3389/fnagi.2016.00175
80. Bian Y, Zhao X, Li M, Zeng S, Zhao B (2013) Various roles of astrocytes during recovery from repeated exposure to different doses of lipopolysaccharide. Behav Brain Res 253:253–261. https://doi.org/10.1016/j.bbr.2013.07.028
81. Maggio N, Shavit-Stein E, Dori A, Blatt I, Chapman J (2013) Prolonged systemic inflammation persistently modifies synaptic plasticity in the hippocampus: modulation by the stress hormones. Front Mol Neurosci 6:46. https://doi.org/10.3389/fnmol.2013.00046
82. Sheppard O, Coleman MP, Durrant CS (2019) Lipopolysaccharide-induced neuroinflammation induces presynaptic disruption through a direct action on brain tissue involving microglia-derived interleukin 1 beta. J Neuroinflammation 16(1):106. https://doi.org/10.1186/s12974-019-1490-8
83. Barter J, Kumar A, Stortz JA, Hollen M, Nacionales D, Efron PA, Moldawer LL, Foster TC (2019) Age and sex influence the hippocampal response and recovery following sepsis. Mol Neurobiol 56: 8557–8572. https://doi.org/10.1007/s12035-019-01681-y
84. Chung WS, Clarke LE, Wang GX, Stafford BK, Sher A, Chakraborty C, Joung J, Foo LC et al (2013) Astrocytes mediate synapse elimination through MEGF10 and MERTK pathways. Nature 504(7480):394–400. https://doi.org/10.1038/nature12776
85. Barter JD, Foster TC (2018) Aging in the brain: new roles of epigenetics in cognitive decline. Neuroscientist:1073858418780971. https://doi.org/10.1177/1073858418780971